Materials and Design 54 (2014) 72–78

Contents lists available at ScienceDirect

Materials and Design

journal homepage: www.elsevier.com/locate/matdes

Age hardening behaviors, mechanical and corrosion properties of deformed Mg–Mn–Sn sheets by pre-rolled treatment

Daqing Fang [a,b], Ning Ma [a], Kangle Cai [a,b], Xuecheng Cai [a], Yuesheng Chai [b], Qiuming Peng [a,*]

[a] State Key Laboratory of Metastable Materials Science and Technology, Yanshan University, Qinhuangdao 066004, PR China
[b] School of Materials Science and Engineering, Taiyuan University of Science and Technology, Taiyuan 030024, PR China

ARTICLE INFO

Article history:
Received 23 May 2013
Accepted 9 August 2013
Available online 19 August 2013

Keywords:
Magnesium alloys
Age hardening behavior
Cold rolling
Precipitation strengthening

ABSTRACT

The age behaviors, mechanical and corrosion properties of Mg–1.5Mn–*x*Sn (*x* = 1 and 5 wt.%) alloys under three aging conditions have been investigated. The results reveal that both age behaviors and mechanical properties are improved with the increment of Sn. Meanwhile, the mechanical properties of EA (extrusion + artificial aging) state Mg–1.5Mn–5Sn alloy are higher than those of SA (solid solution + artificial aging) state sample, which are mostly attributed to fine grain and high density secondary precipitate. In addition, an accompanying improvement in age hardening response and strength is achieved in ERA (extruded + rolled + aging) state alloy compared with EA state one. The main reasons are related to the formations of a large number of dislocations and deformation twins, which provide effective nucleation sites to form fine β-Mg_2Sn strengthening precipitates during the following aging process. In addition, compared with EA state sample, a lower corrosion rate of ERA alloy is confirmed by Tafel curves and electrochemical impedance spectroscopy results, which is mainly related to the formation of a thick anodic passivation film on the surface.

1. Introduction

Mg–Sn system exhibits a great deal of potential advantages to develop high performance Mg alloys [1,2]. First of all, the maximum solid solubility of Sn in Mg matrix is 14.85 wt.% at the eutectic temperature of 561 °C, and it changes to 0.85 wt.% at 200 °C [3]. Thus, the mechanical properties can be improved by age strengthening. Secondly, Mg_2Sn precipitate (melting point: 770 °C) has higher thermal stability compared with other strengthening particles, such as $Mg_{17}Al_{12}$ phase or the precipitates containing rare earth elements (REs) [4,5]. And then both the mechanical properties at elevated temperatures and creep resistance can be enhanced simultaneously. Thirdly, the addition of Sn is regarded as an effective alloying element to substitute partial REs due to their similar strengthening mechanisms [6]. Additionally, its low cost is of particular attraction to expand their applications of heat resistant Mg alloys in the future [7].

More recently, extensive researches have been performed on Mg–Sn based system. For example, Liu et al. [8] found that the compressive creep resistance of Mg-5 wt.% Sn alloy is improved due to the dispersive Mg_2Sn phase. The presence of stable nanoparticles increases the resistance to dislocation movement, leading to the improvement of creep resistance. Whereafter, it is reported that age hardening response and mechanical properties of Mg–Sn based alloys can be improved by adding Zn because of the formation of submicron $MgZn_2$ and Mg_2Sn particles [9]. Sasaki et al. [1,10] investigated the double aging and micro-alloying on the age hardening behavior of Mg-Sn-Zn alloy and found different morphologies of Mg_2Sn precipitate under different treatment conditions. A plate-like precipitate with the orientation relationship (OR) of $(0001)_{Mg}\|(1\bar{1}0)_{Mg2Sn}$, $[11\bar{2}0]_{Mg}\|[1\bar{1}1]_{Mg2Sn}$ and a rod-like precipitate with the OR of $(0001)_{Mg}\|(111)_{Mg2Sn}$, $[11\bar{2}0]_{Mg}\|[1\bar{1}2]_{Mg2Sn}$ are detected after aging at 200 °C. A rod-like precipitate and a lath-like one with the OR of $(0001)_{Mg}\|(1\bar{1}0)_{Mg2Sn}$, $[11\bar{2}0]_{Mg}\|[001]_{Mg2Sn}$ are presented when it is aged at 160 °C [1]. However, a refining polygonal precipitate is observed with the OR of $(0001)_{Mg}\|(111)_{Mg2Sn}$, $[11\bar{2}0]_{Mg}\|[\bar{1}01]_{Mg2Sn}$ after the double aging treatment, which improves the peak hardness. More attractively, high ductility and even superplastic deformation behavior are achieved in Mg–Sn–Zn based alloys by tailoring the morphology and size of strengthening precipitate [10].

Up to now, it is established that the formation of secondary precipitates in Mg–Sn based alloys plays an important role in determining the mechanical properties. Although both strength and deformability are improved, there still exist some shortcomings restraining their applications. For instance, it frequently takes a long time to reach the peak hardness at elevated temperatures, which results in the vast depletion of energy and the coarsening of strengthening precipitates [7,11]. In addition, in contrast to

* Corresponding author. Tel.: +86 335 8057047; fax: +86 335 8074545.
E-mail address: pengqiuming@ysu.edu.cn (Q. Peng).

0261-3069/$ - see front matter © 2013 Elsevier Ltd. All rights reserved.
http://dx.doi.org/10.1016/j.matdes.2013.08.028

the strengthening phase along the $\{11\bar{2}0\}_{Mg}$ prismatic plane, those distributes along $\{0001\}_{Mg}$ basal plane provide weaker strengthening effect [12]. In addition, the addition of Sn is significantly associated with the corrosion properties of Mg–Sn based alloys. Song [13] found that Sn modification significantly decreases the susceptibility of localized corrosion attack. The corrosion mode and corrosion rate were associated with the quantity of Mg_2Sn phases and tin concentration of the matrix [14]. Therefore, the optimizing of age approach, together with the interpreting of the relationship between strengthening phase and corrosion properties, become critical issues to develop Mg–Sn based alloys.

In this study, a pre-rolled treatment before aging has been established as an effective method to shorten aging time and increase the volume fraction of strengthening precipitate simultaneously. The comparative investigations have been performed among three aging treatments. The microstructures, age behaviors and corrosion resistance properties of Mg–Sn based alloys have been studied in detail.

2. Experimental process

Two plate-shaped Mg–1.5Mn–*x*Sn (*x* = 1 and 5 wt.%) ingots with $90 \times 30 \times 200\ mm^3$ were prepared by gravity casting technique. These samples were solid solution treated at 480 °C for 10 h and then artificial aging at 200 °C from 10 to 100 h (SA state). In addition, the solid solution samples were pre-heated at 300 °C for 1 h and then hot extruded into plates with a thickness of 8 mm and a width of 50 mm. After extrusion, the corresponding samples were aged at 200 °C for the same time (EA state). Comparatively, the as-cast sample was solid solution treated and extruded under the same condition as above process. Subsequently, the plates were rolled at room temperature parallel to the extrusion direction. The reduction per pass was restricted to 2%, meanwhile, the sheet was reversed 180°between passes. The final thickness was 7.5 mm. The sheets were aged at 200 °C for the same time (ERA state: extruded + rolled + aging).

Microstructure investigations were performed using optical microscopy (OM) and transmission electron microscopy (TEM). The optical microstructures of deformed samples were observed along the extruded direction (ED) or the rolled direction (RD). The grain sizes were measured using the linear intercept method. The standard procedures including grinding, polishing and etching were applied. The TEM specimens were thinned using twin-jet method at a voltage of 30 V with a working temperature of −30 °C. The twin-jet solution included 6% vol.% perchloric acid ethanol solution.

The phase compositions were identified by X-ray diffraction with Cu Kα radiation at a scan rate of 0.1 °/s. Microhardness was measured by Vickers hardness tester. The load and the dwelling time were 100 gf and 15 s, respectively. Tensile tests were conducted using Instron machine at room temperature with an initial strain rate of $1 \times 10^{-3}\ s^{-1}$.

Electrochemical tests were carried out using a Bio-logic VSP potentiostat/frequency response analysis system to evaluate the electrochemical behaviors. Experiments were carried out in a three-electrode electrochemical cell, with a saturated calomel electrode (SCE) as the reference electrode, a platinum mesh as counter electrode and the investigated specimen as the working electrode. The experiments were carried out in 0.9 wt.% NaCl aqueous solutions at a temperature of 25 ± 1 °C. The polarization curves of two alloys were obtained by exposing them into corrosion media. The electrochemical impedance spectroscopy (EIS) was carried out at open potential with the amplitude of 10 mV over the frequency range of 100 kHz–0.1 Hz. The specimens were exposed to the corrosion media at different times, viz., 2, 4, 6, 8 and 12 h to investigate the mechanism. The EC-Lab software was employed to fit the EIS by the equivalent circuit.

3. Results

The age responses of Mg–1.5Mn–*x*Sn alloys in different states are shown in Fig. 1. In the case of Mg–1.5Mn–1Sn alloy, age hardening response is hardly observed after SA treatment. The relatively stable value of 38 HV is maintained during the whole aging period. Compared with SA treatment, the same tendency is detected while the corresponding hardness is improved after EA treatment. In contrast to the EA state, the main discrepancy after ERA treatment resides in the improved solid-solution hardness (SHV), which changes from 44 HV to 50 HV. Nevertheless, the comparable values are observed when the aging time is over 30 h.

As far as Mg–1.5Mn–5Sn alloy is concerned, a significant age hardening behavior is achieved after SA treatment. Namely, the hardness keeps stable at the beginning of the aging process. And then it increases with the increment of aging time. The peak hardness (PHV) of 63 HV is observed after aging for 76 h, which is 1.22 times higher than SHV. The main difference between SA and EA treatments is that the time reaching the PHV is shortened to 48 h and the PHV changes to 65 HV. However, it is worth noting that both the PHV and the aging time to the PHV are improved after ERA treatment. It merely takes 24 h to arrive the PHV of 75 HV. The aging time of the ERA condition is 50% of that under EA treatment.

Fig. 2 shows the optical microstructures of Mg–1.5Mn–5Sn samples under different states at PHV. The SA state sample (Fig. 2a) is mostly composed of equiaxed grains and smooth grain boundaries. The average grain size (AGS) fluctuates greatly. The value is around 147 ± 20 μm. For the EA state alloy (Fig. 2b), the alloy consists of regular polygon grains owing to the dynamic recrystallization. The fine secondary phases are mostly distributed along the grain boundaries. The value of AGS is about 38 ± 2 μm. The similar microstructure is observed in the ERA alloy as that of the EA state one. However, there are a number of twins on the surface formed during the cool rolling process. Meanwhile, the grain boundaries are severely deformed along the rolling direction. Fig. 3 shows the XRD patterns of different state Mg–1.5Mn–5Sn specimens, where the alloys under three different conditions are primarily composed of α-Mg and Mg_2Sn phases. The peak positions of ERA state sample shift toward low angle direction compared with SA and EA ones.

TEM bright field graphs and selected area electron diffraction (SAED) patterns of different state Mg–1.5Mn–5Sn samples at PHV are shown in Fig. 4. The average size of rod-like precipitate in the

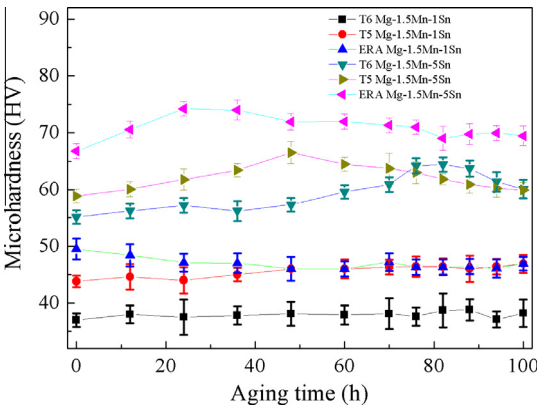

Fig. 1. The aging curves of Mg–1.5Mn–*x*Sn alloys under different conditions.